



Shape and surface properties of titanate nanomaterials influence differential cellular uptake behavior and biological responses in THP-1 cells



Suwimon Boonrungsiman^a, Wongsakorn Suchaoin^a, Paninee Chetprayoon^a, Nawin Viriyapempikul^b, Sasitorn Aueviriyavit^a, Rawiwan Maniratanachote^{a,*}

^a Nano Safety and Risk Assessment Laboratory, National Nanotechnology Center (NANOTEC), National Science and Technology Development Agency (NSTDA), 111 Thailand Science Park, Khlong Luang, Pathum Thani 12120, Thailand

^b Nanomaterials for Energy and Catalysis Laboratory, National Nanotechnology Center (NANOTEC), National Science and Technology Development Agency (NSTDA), 111 Thailand Science Park, Khlong Luang, Pathum Thani 12120, Thailand

ARTICLE INFO

Keywords:

Cellular uptake
Inflammatory response
Surface pH
THP-1
Titanate nanofibers
Titanate nanomaterials

ABSTRACT

We investigated cellular uptake behavior and biological responses of spherical and fibrous titanate nanomaterials in human monocyte THP-1 cells. Two titanate nanofibers (TiNFs), namely TF-1 and TF-2, were synthesized from anatase TiO₂ nanoparticles (TNPs) via hydrothermal treatment. The synthesized TiNFs and TNPs were thoroughly characterized for their size, crystallinity, surface area and surface pH. TF-1 (~2 μm in length) was amorphous with an acidic surface, while TF-2 (~7 μm in length) was brookite with a basic surface. The results demonstrated that none of these titanate nanomaterials resulted in significant cytotoxicity, even at the highest doses tested (50 μg/ml), consistent with an absence of ROS generation and lack of change of mitochondrial membrane potential. While no cytotoxic effect was found in the titanate nanomaterials, TF-2 tended to decrease the proliferation of THP-1 cells. Furthermore, TF-2 resulted in an inflammatory cytokine response, as evidenced by dramatic induction of IL-8 and TNF-α release in TF2 but not TF-1 nor TNPs. These results suggest that shape of titanate nanomaterials plays an important role in cellular internalization, while surface pH may play a prominent role in inflammatory response in THP-1 cells.

1. Introduction

TiO₂ or titanate nanomaterials have been used in various applications due to their unique and versatile properties, and ability to be processed into various shapes, including nanoparticles, nanofibers and nanotubes. The risk of human exposure to TiO₂ nanoparticles (NPs) from consuming products and occupational activities arises as a consequence. TiO₂ has been known to be chemically inert and biologically non-toxic in its bulk state. However, the physicochemical behavior and biological properties of materials can change dramatically as particles approach nanoscale dimensions. It is known that ultrafine particulate matters with dimensions below 200 nm can readily enter the human body via inhalation or ingestion and subsequently distribute throughout the body [1,2]. A number of reports demonstrated toxicity of TNPs in various cell types, in which the main underlying mechanism of toxicity was TNP-mediated intracellular reactive oxygen species (ROS) production and subsequent apoptosis [3,4]. On the other hand, other reports showed no or very low toxic effects of TNPs on cells even at elevated concentrations [5]. Conflicting reports on the toxicological

effects of TNPs could be explained by different sources of materials, cell types, and experimental designs used in each study. Therefore, it is critical that physicochemical characteristics of nanomaterials, such as size, shape, crystalline phase and surface activity be determined in parallel with the biological effects [1].

Fiber-shaped TiO₂, or titanate nanofibers (TiNFs), have been increasingly used in photocatalysts [6], material coating and reinforcements [7] and scaffold for medical applications [8]. For safety aspects, TiNFs with larger aspect ratio have been reported to promote higher cytotoxic responses. In mice, the longer TiNFs triggered higher pulmonary inflammatory responses than shorter ones [9]. While the number of novel engineered titanate nanomaterials has been rapidly increased, it is still unclear whether these nanomaterials represent a significant risk to human and environmental exposure.

To address whether titanate nanomaterials are toxic and what physical or chemical properties mediate their toxicity, we synthesized two distinct forms of TiNFs from TNPs by hydrothermal treatment and performed a set of physicochemical characterization. These two TiNFs exhibited a different length and surface pH. The nanomaterials were

* Corresponding author.

E-mail address: rawiwan@nanotec.or.th (R. Maniratanachote).

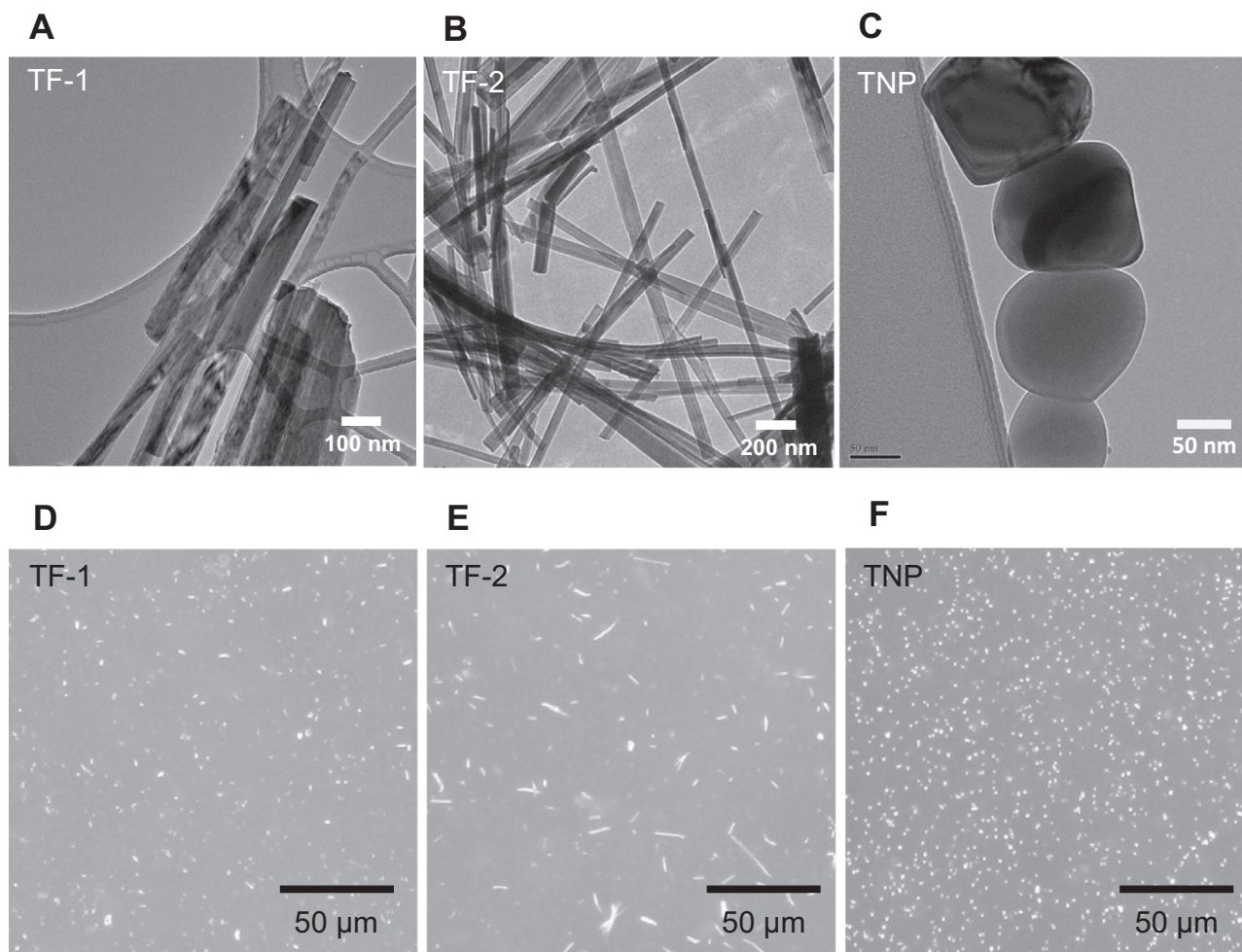


Fig. 1. Morphological analyses of titanate nanomaterials. Titanate nanomaterials were dispersed in distilled water at a concentration of 1 mg/ml. TF-1 (A), TF-2 (B), and TNP (C) were analyzed with TEM. To see morphological characteristics of the nanomaterials when they are dispersed in cell culture media, 1 mg/ml of titanate nanomaterials suspension were further diluted with culture media to a final concentration of 25 $\mu\text{g/ml}$. TF-1 (D), TF-2 (E), and TNP (F) were visualized using a digital optical microscope.

Table 1
Primary size, surface area and surface pH of titanate nanomaterials.

Sample	TF-1	TF-2	TNP
Primary size ^a (nm)	54 \pm 31	73 \pm 21	170 \pm 51
Hydrodynamic diameter			
● In water (nm)	373 \pm 10	639 \pm 5	353 \pm 1
● In RPMI ^b (nm)	447 \pm 48	810 \pm 126	530 \pm 15
Zeta potential			
● In water (mV)	-45.23 \pm 0.91	-51.17 \pm 0.75	-11.47 \pm 1.1
● In RPMI ^b (mV)	-10.83 \pm 0.57	-10.22 \pm 1.02	-9.43 \pm 0.67
Fiber length ^c (μm)	2.3 \pm 0.6	7.4 \pm 2.7	n.d.
Surface area (m^2/g)	35	29	8
Surface pH ^d	1.2–2.9	10.6–12	2.9–3.0
pH			
● In water	7.75	9.51	7.35
● In RPMI ^b	7.86	7.91	7.84

n.d., not defined.

^a Diameter of TiNFs as measured from TEM images.

^b Complete culture media.

^c Fiber length as measured from 3D optical microscope images.

^d Acid-base strength analysis using Hammett indicators.

then investigated for their uptake behavior and cellular responses in THP-1 cells, a human monocytic cell line extensively used to study macrophage function. This study demonstrated that the aspect ratio and surface properties of titanate nanomaterials influence cellular uptake and biological responses of the cells.

2. Materials and methods

2.1. Nanomaterial synthesis

TNPs (anatase, surface area=8 m^2/g) (Kishida, Osaka, Japan) were used as a precursor to synthesize TiNFs by a hydrothermal process as previously described [10]. Briefly, 0.5 g of TiO_2 in 50 ml of 10 M NaOH aqueous solution was sonicated for 8 min by a titanium horn in a Teflon vessel. Sonication power supplied to the solution was controlled at 0 and 7.6 W to produce two distinct forms of TiNFs, designated as TF-1 and TF-2, respectively. After hydrothermal treatment in an oven at 180 $^\circ\text{C}$ for 3 days, samples were filtrated and treated with 0.1 M HCl solution. The obtained TiNFs were washed with distilled water until pH of the wash reached 7, and dried at 70 $^\circ\text{C}$ in an oven.

2.2. Nanomaterial characterization

Crystallinity of titanate nanomaterials was characterized by X-ray diffraction (XRD) measurement (RINT 2000, Rigaku, Tokyo, Japan) using $\text{Cu K}\alpha$ radiation ($\lambda=1.5406 \text{ \AA}$) and a step size of 0.02 $^\circ$. Specific surface area was determined from nitrogen sorption (BelSorp-Mini II, BEL Japan Inc., Japan). Surface pH was evaluated by Hammett indicators. The reagents 4-(phenylazo) diphenylamine, methyl yellow, bromo phenol blue, thymolphthalein, and alizarin yellow were dropped onto surface of the samples and kept in the closed vessel for 1 d to investigate the indicator color (i.e. acid-basic strength) [11].

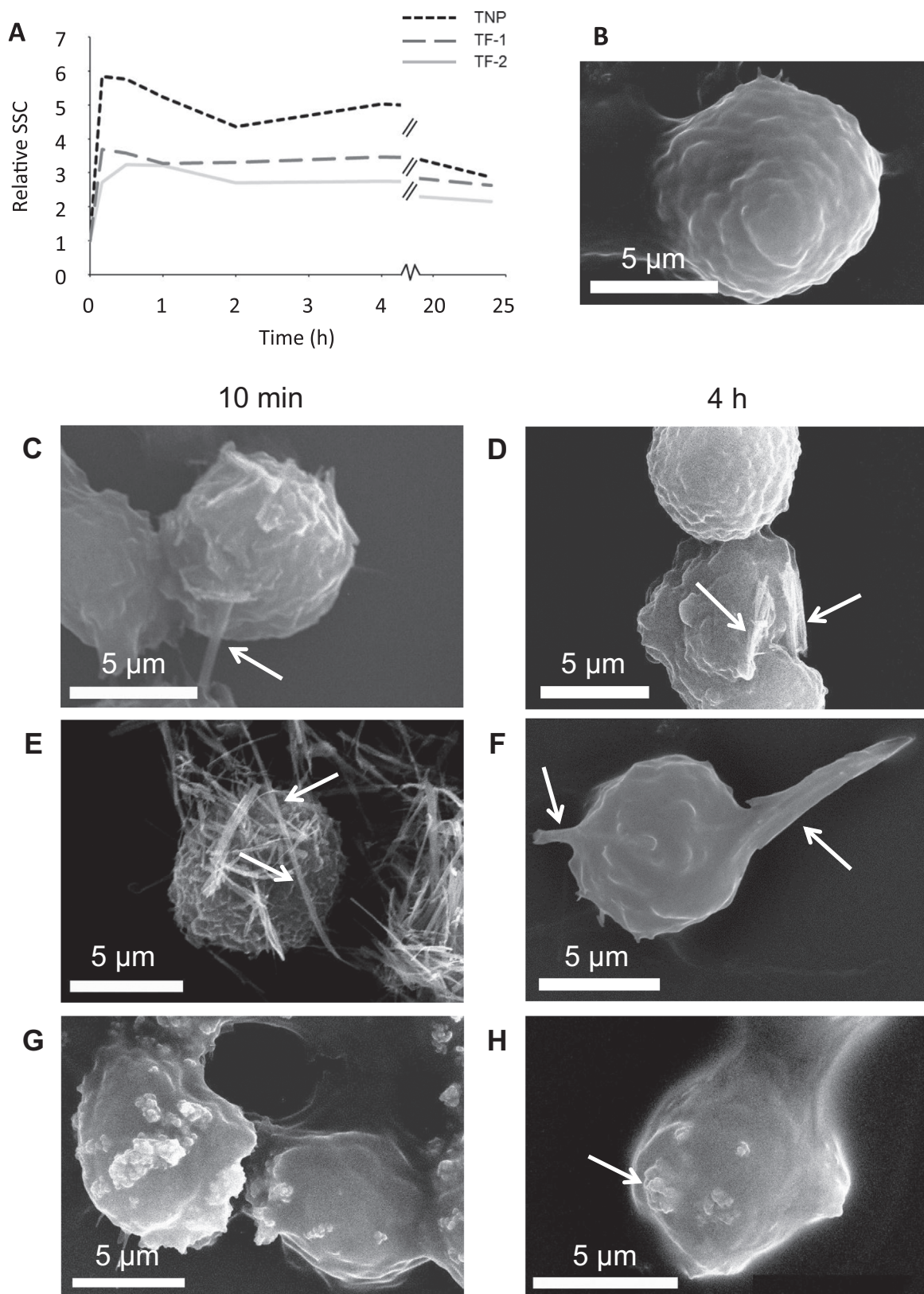


Fig. 2. Uptake of titanate nanomaterials by THP-1 cells. THP-1 cells were treated with 25 µg/ml titanate nanomaterials for 24 h. (A) SSC of the samples were measured using a flow cytometer. (B–H) For SEM analyses, non-treated THP-1 cells (B), were compared with THP-1 cells treated with titanate nanomaterials TF-1 (C and D), TF-2 (E and F) and TNP (G and H) at 10 min and 4 h, respectively. White arrows indicate the presence of titanate nanomaterials. The scale bars are 5 µm.

Primary sizes of titanate nanomaterials were determined from transmission electron microscopy (TEM, JEOL 2100, Tokyo, Japan). Nanomaterials were dispersed in distilled water at a concentration of

1 mg/ml, sonicated for 10 min and dropped onto a lacey grid. Diameters of nanomaterials were measured from 200 pieces of each type.

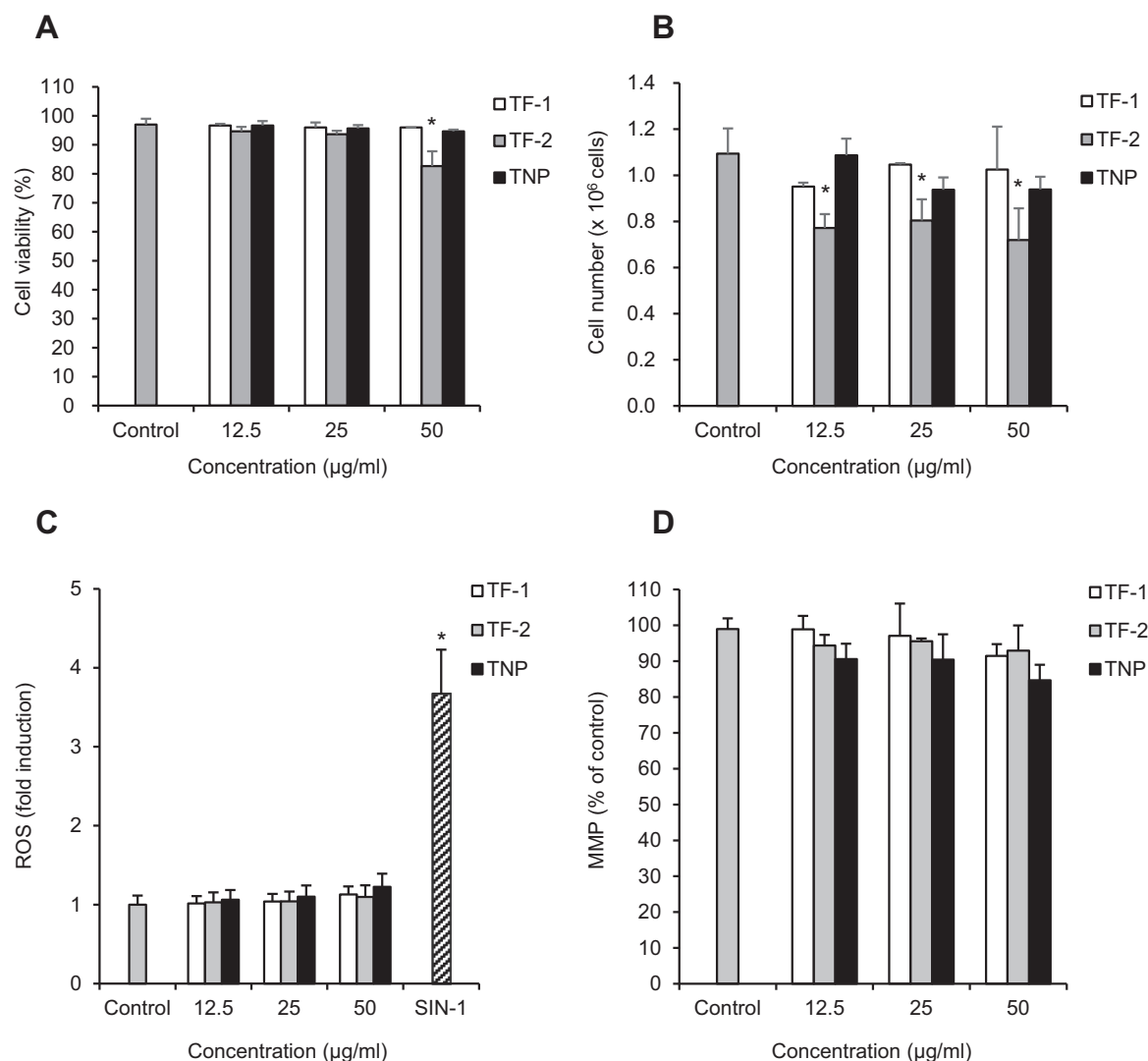


Fig. 3. Cellular response of THP-1 cells to titanate nanomaterials. The cells were exposed to TF-1, TF-2 and TNP at concentrations of 0–50 µg/ml for 24 h. (A) Cell viability was evaluated by the trypan blue exclusion assay. (B) Total live cell counts for trypan blue stained THP-1 cells. (C) Intracellular ROS production was evaluated by the DCF assay. SIN-1 solution (0.5 µg/ml) was used as a positive control for the DCF assay. (D) Change of MMP as analyzed by the TMRE assay. Cells treated without nanomaterials (0 µg/ml) serve as a control. The asterisk denotes statistical significance by a two-tailed Student's *t*-test relative to the control ($p < 0.05$).

In addition, nanomaterials in distilled water (1 mg/ml, sonication for 10 min) and their dilution in complete culture media (100 µg/ml) were subjected for hydrodynamic size and zeta potential analyses, using a dynamic light scattering (DLS, Malvern Zetasizer Nano, UK).

2.3. Cell culture and sample preparation

THP-1 cells (ATCC, Manassas, VA) were cultured in RPMI-1640 (Sigma, St. Louis, MO) supplemented with 10% FBS (Invitrogen, Carlsbad, CA) at 37 °C in 5% CO₂ humidified environment. Titanate nanomaterials (TNP, TF-1 and TF-2) were sterilized in hot air oven at 180 °C for 3 h. The materials were dispersed as a stock suspension (1 mg/ml) in sterile water, sonicated for 10 min, and then serially diluted with sterile water to 10X of required final concentrations. Hence, these suspensions were used 10% v/v in cell culture media for treating the cells. An equal volume of sterile water without nanomaterials was used as a control. The experiments were carried out in an absence of UV light in order to avoid the interference of potential photocatalytic activity of titanate nanomaterials. 6×10^5 THP-1 cells in a 12-well plate were used in all experiments unless otherwise specified.

2.4. Side scatter (SSC) analysis

THP-1 cells were exposed to nanomaterials at a concentration of 25 µg/ml. The treated cells were collected at different time points from 0, 10, 30 min, and 2, 4, and 24 h. The laser scattering of treated cells was analyzed by a flow cytometer (FACSaria II, BD Biosciences, Franklin Lakes, NJ).

2.5. Sample preparation for scanning electron microscope (SEM) analysis

THP-1 cells were incubated with titanate nanomaterials at a concentration of 25 µg/ml. The cells were collected at 10 min and 4 h, and fixed with 4% glutaraldehyde (Sigma) in 0.1 M PIPES buffer at 4 °C for 2 h. All samples were then dehydrated in a graded ethanol series from 50%, 70%, 90% and 100% v/v, followed by coating with hexamethyldisilazane (HDMS), and dried in an ambient atmosphere. The samples were sputter coated with gold before imaging by SEM (Hitachi S-340N, Tokyo, Japan).

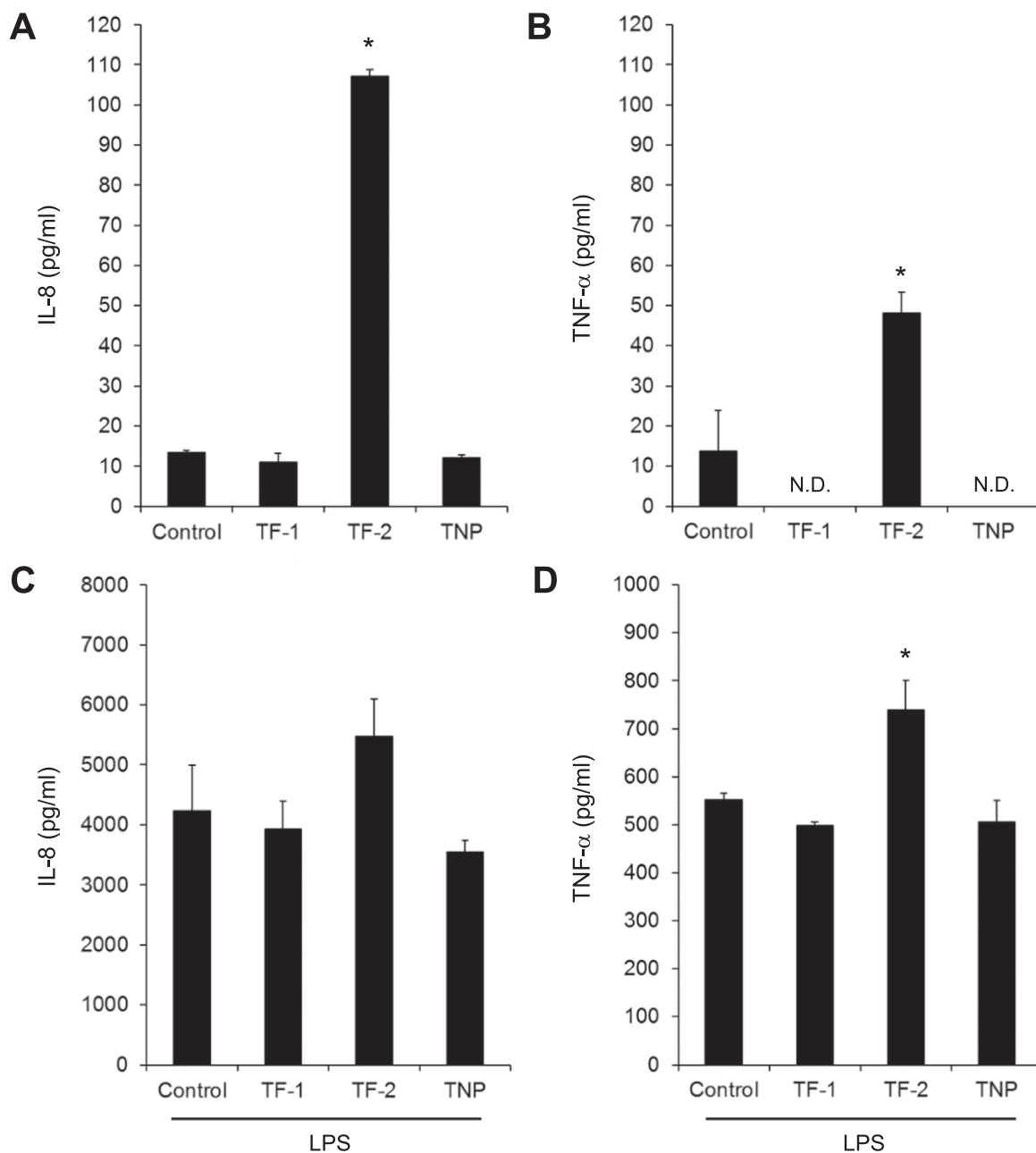


Fig. 4. Effects of titanate nanomaterials on release of inflammatory cytokines by THP-1 cells. THP-1 cells were exposed to TF-1, TF-2, or TNP at a concentration of 25 $\mu\text{g}/\text{ml}$ for 24 h. IL-8 (A, C) and TNF- α (B, D) were analyzed by ELISA. LPS (0.1 $\mu\text{g}/\text{ml}$) was used as a co-stimulant together with titanate nanomaterials (C, D). N.D. indicates that the cytokine concentration is below the detection limit and therefore could not be determined. The asterisk denotes statistical significance by a two-tailed Student's *t*-test relative to the control ($p < 0.05$).

2.6. Sample preparation and TEM analysis

THP-1 cells were treated with titanate nanomaterials as described in SEM analysis. The cells were collected at 24 h after exposure, fixed with 4% glutaraldehyde in 0.1 M PIPES buffer at 4 $^{\circ}\text{C}$ for 2 h, then post-fixed in 1% v/v osmium tetroxide in 0.1 M PIPES buffer at room temperature for 1 h. The specimens were dehydrated in a graded series of ethanol from 50%, 70%, 90% and 100% v/v, and progressively infiltrated in the Epon 812 (32.5 Epon 812, 20 ml DDSA, 17.5 MNA and 1.3 ml DMP-30) with resin:ethanol ratios of 1:3, 1:2, 2:1, and purified resin for 3, 3, 24 and 6 h, respectively. Finally, the specimens were transferred to fresh resin and polymerized at 65 $^{\circ}\text{C}$ for 24 h. The embedded samples were cut using an ultramicrotome. A70 nm-thick section was collected on 300-mesh copper grid for TEM analysis.

2.7. Determination of particle size in culture media

Because of the known limitation of DLS in accurately measuring dimensions of high aspect ratio particles like fibrous materials, the particles sizes of titanate nanomaterials were visualized in culture media. TiNFs and TNPs were dispersed in ultrapure water at the concentration of 1 mg/ml, sonicated for 10 min, and diluted in complete culture media to a final concentration of 25 $\mu\text{g}/\text{ml}$. The suspension was dropped onto a glass slide and visualized by a digital optical microscope (DSX510, Olympus, Tokyo, Japan). The length of TiNFs and the diameter of TNPs were measured from 30 particles each and averaged.

2.8. Evaluation of cytotoxicity

Cytotoxicity was investigated by trypan blue exclusion, since titanate nanomaterials have been reported to interfere the MTT result [12]. THP-1 cells were seeded at a density of 5×10^4 cells/well in a 96-well plate, and exposed to various concentrations of titanate nanomaterials (0–50 $\mu\text{g/ml}$) for 24 h. 10 μl of cell suspension was stained with 10 μl of trypan blue solution. Live and total cell counts were evaluated by an automated cell counter (TC20™, Bio-Rad, Hercules, CA). Percentage cell viability was determined by dividing total number of living cells by the total number of cells counted.

2.9. Detection of intracellular ROS

THP-1 cells were incubated in 50 μM of 2',7'-dichlorodihydrofluorescein diacetate ($\text{H}_2\text{DCF-DA}$, Sigma) for 40 min, washed twice with pre-warmed HBSS (Hank's Balanced Salt Solution), and transferred to a black 96-well plate at a density of 5×10^4 cells/well. The cells were then exposed to various concentrations of titanate nanomaterials (0–50 $\mu\text{g/ml}$) for 3 h. At the end of incubation time, fluorescence intensity was measured using a SpectraMax® M2 microplate reader (Molecular Devices, Sunnyvale, CA) with excitation and emission wavelengths of 485 nm and 528 nm, respectively. A 0.5 μM of 3-morpholino-sydnimine (SIN-1, Sigma) was used as a positive control.

2.10. Mitochondrial membrane potential (MMP) analysis

MMP was analyzed by staining with tetramethylrhodamine ethyl ester (TMRE, Sigma) after exposure to titanate nanomaterials. In this experiment, THP-1 cells were incubated with various concentrations of titanate nanomaterials (0–50 $\mu\text{g/ml}$) for 24 h. At the end of exposure, cells were washed twice with PBS, incubated with 25 nM TMRE solution at 37 °C for 15 min while protected from light exposure, and subsequently washed twice with PBS. Ten thousand cells were analyzed for TMRE fluorescence signal accumulated in the mitochondria using a flow cytometer. Measurement was done at excitation and emission wavelengths of 488 nm and 560 nm, respectively. The acquired data was analyzed using the BD FACSDiva software.

2.11. Measurement of released cytokines

THP-1 cells were exposed to 25 $\mu\text{g/ml}$ titanate nanomaterials for 24 h. Lipopolysaccharide (LPS, Sigma) was used as co-stimulant with nanomaterials. IL-8 and TNF- α were measured in cell culture media using an enzyme-linked immunosorbent assay (ELISA, PeproTech, Rocky Hill, NJ) according to manufacturer's instructions.

2.12. Statistical analysis

Data were presented as the mean \pm standard deviation (SD) of three independent experiments. Significant differences among groups were analyzed by one-way analysis of variance (ANOVA) using Dunnett's post hoc test. The level of statistical significance was $p < 0.05$.

3. Results

3.1. Nanomaterial synthesis and characterization

TEM images (Fig. 1A–C) showed fibrous shapes for the two synthesized TiNFs, TF-1 and TF-2, and a spherical shape of the precursor TNPs. The X-ray diffraction (XRD) pattern suggested that TNPs, TF-1 and TF-2 were anatase, amorphous and brookite, respectively (Supplementary Fig. S1). In RPMI, the absolute values of zeta potential of all nanomaterials were reduced, due to their interactions with biomolecules in the culture media. The hydrodynamic size of TF-2 was about two times larger than that of TF-1, in both distilled water

and RPMI (Table 1). The DLS technique might be not suitable for measuring the size of nanomaterials, which have high aspect ratio, like TiNFs. However, the DLS analysis is useful in examining the hydrodynamic behavior of TF-1 and TF-2 when dispersed in culture media. After dispersion in cell culture media, TF-1 and TF-2 were viewed under a 3D optical microscope and exhibited approximate lengths of $2.3 \pm 0.6 \mu\text{m}$ and $7.4 \pm 2.7 \mu\text{m}$, respectively (Fig. 1D and E), while TNPs exhibited a spherical shape (Fig. 1F). Similar results were observed when TiNFs and TNPs were dispersed in distilled water (data not shown). From the acid-base strength analysis, surface pH of TF-1 and TNPs was acidic, while that of TF-2 was basic. However, none of them caused changes in the pH of exposure media due to the buffering capacity of the media (Table 1).

3.2. Phagocytic uptake of titanate nanomaterials by THP-1

SSC patterns reflecting cellular granularity due to the presence of intracellular titanate nanomaterials were investigated. After exposing THP-1 cells to nanomaterials, all SSC patterns increased within the first 10 min (Fig. 2A). The SSC patterns of TF-1 and TF-2 were similar, whereas TNPs showed the highest SSC pattern for at least 4 h. At 24 h of exposure, the SSC patterns for all nanomaterials were comparable (Fig. 2A). SEM images revealed that TF-1, TF-2 and TNPs associated with the cell membrane within the first 10 min of exposure (Fig. 2C, E and G). After 4 h of exposure, the particles were mostly internalized, demonstrating that all three titanate nanomaterials can be taken up by THP-1 cells (Fig. 2D, F and H). In addition, TF-2 resulted in a strikingly irregular morphology of the cells due to the TF-2 fibrous shape (Fig. 2F). The internalization and localization of these titanate nanomaterials were confirmed by TEM, which demonstrated the localization of TF-1, TF-2 and TNPs in THP-1 cells after 24 h of exposure (Supplementary Fig. S2). Most of the individual particles were found inside vesicles, while some of them were observed in the cytoplasm with an absence of surrounding membrane bound structure (Supplementary Fig. S2-C and S2-D).

3.3. Cytotoxic responses in THP-1 caused by titanate nanomaterials

Using the trypan blue exclusion assay, the cell viability of THP-1 treated with all titanate nanomaterials was higher than 80% after 24 h of exposure (Fig. 3A). While treatment with TF-1 and TNPs did not give significant changes in cell number, the number of living cells was found to be lower in TF-2 treatment at all concentrations, indicating lower cell proliferation (Fig. 3B). At the investigated concentrations, all of these nanomaterials did not induce ROS generation, one of the common mechanisms of cell death induced by NPs (Fig. 3C). Next, the level of intracellular free radicals was evaluated by measuring the membrane potential of mitochondria. In agreement with the lack of ROS, none of these titanate nanomaterials caused significant loss of MMP (Fig. 3D). Previous studies also showed that anatase and rutile forms of TiO_2 nanoparticles did not generate intracellular ROS in A549 cells at concentrations below 100 $\mu\text{g/ml}$ [5].

3.4. Induction of inflammatory responses in THP-1 by titanate nanomaterials

The release of pro-inflammatory factors, IL-8 and TNF- α , was measured to evaluate the inflammatory response. It was found that TF-2 significantly induced both IL-8 and TNF- α release (107.17 ± 1.7 and $48.25 \pm 5.10 \text{ pg/ml}$, respectively) compared to the untreated cells (13.44 ± 0.45 and $13.66 \pm 10.12 \text{ pg/ml}$, respectively) (Fig. 4A and B). Similarly, treatment of TF-2 together with LPS induced the highest level of both inflammatory factors ($5467.84 \pm 629.13 \text{ pg/ml}$ for IL-8 and $739.30 \pm 61.49 \text{ pg/ml}$ for TNF- α) (Fig. 4C and D). In comparison, TF-1 and TNPs treatments did not significantly induce or suppress the production of IL-8 and TNF- α in the presence of LPS.

4. Discussion

There have been a number of studies on the effects of particle length on the biological responses of innate immune cells to NP exposure [13]. Elongated fibrous structure (low specific surface area and high aspect ratio) of NPs has been proposed to be critical to cellular toxicity. For example, longer TiNFs have been reported to induce higher cytotoxicity [14]. In the present study, whilst the viability of THP-1 monocytic cells exposed to all titanate nanomaterials at concentrations up to 50 µg/ml was higher than 80% with no detectable ROS generation, TF-2 at all concentrations tended to reduce cell proliferation. Moreover, TF-2 exposure resulted in significantly higher IL-8 and TNF-α release, suggesting that TF-2 induces an inflammatory response in THP-1 cells. These results suggest that the aspect ratio is involved in the inflammatory responses of THP-1.

The release of inflammatory cytokines observed in TF-2 was likely triggered by the uptake of large particles by THP-1 cells. THP-1 exhibited an irregularly extended shape after phagocytosis of TF-2 (Fig. 2F). This phenomenon, also known as “frustrated phagocytosis”, occurs when the size of target is too large to be engulfed, and is usually found in the uptake of particularly long particles such as asbestos, leading to incomplete clearance and inflammation [15]. The phagocytosis of TiO₂ has been reported to stimulate the production of IL-1β in THP-1, and the release of cytokine was lower when phagocytosis was inhibited [16].

Apart from the shape of nanomaterials, which play an important role on the uptake pattern of phagocytic cells, the surface properties of nanomaterials might also have affected the innate immune response. The induction of pro-inflammatory cytokines has been suggested to depend on the surface area of internalized materials as the larger surface area can be more reactive [17]. However, TF-1 exhibited a larger surface area than TF-2 (Table 1) but did not result in cytotoxicity nor release of inflammatory factors. Thus, other surface properties might be associated with a reduction of cellular proliferation and increased inflammatory responses of TF-2.

In our synthesis process, both TF-1 and TF-2 were prepared from the same precursor TNPs. TF-2, but not TF-1, was subjected to sonication which caused a diffusion of Na⁺ and OH⁻ through the inter-particle space, forming an elongated shape [18]. As a consequence, the resulting surface pH of TF-2 was more basic, while TF-1 and TNPs were acidic. The surface pH is known to influence the binding affinity of nanomaterials to ions in the culture media as well as agglomeration and aggregation behaviors of the nanomaterials [18–21]. In light of our findings, the surface pH of titanate nanomaterials might interact with cell membrane during phagocytosis and affect intracellular pH homeostasis after being engulfed. It is possible that after internalization into lysosomes, where highly acidic hydrolytic enzymes are presented, TF-2 particles might trigger inflammatory responses due to a highly basic surface, while on the other hand the lower surface pH of TF-1 and TNPs could suppress cytokine release [22].

So far, there is no comprehensive study regarding the effect of surface pH of nanomaterials on cellular responses. This is an important safety concern for potential medical applications such as drug delivery or implantation. Our results demonstrate that it is critical to perform in-depth physicochemical characterization of nanomaterials in parallel to studies on biological toxicity responses. Furthermore, we conclude that future studies are necessary to better dissect how surface pH and particle dimensions combine to affect toxicological properties of nanoparticles.

Competing interests

The authors declare no competing interests.

Acknowledgements

This work was supported by the Research, Development and Engineering Fund through the National Nanotechnology Center (NANOTEC), NSTDA, Thailand. We thank Dr. Kevin Roy (Department of Genetics, Stanford University, California) for helpful comments and English language review of this manuscript.

Appendix A. Transparency document

Transparency document associated with this article can be found in the online version at <http://dx.doi.org/10.1016/j.bbrep.2016.12.014>.

Appendix B. Supporting information

Supplementary data associated with this article can be found in the online version at <http://dx.doi.org/10.1016/j.bbrep.2016.12.014>.

References

- [1] G. Oberdörster, A. Maynard, K. Donaldson, V. Castranova, J. Fitzpatrick, K. Ausman, J. Carter, B. Karn, W. Kreyling, D. Lai, S. Olin, N. Monteiro-Riviere, D. Warheit, H. Yang, Principles for characterizing the potential human health effects from exposure to nanomaterials: elements of a screening strategy, *Part. Fibre Toxicol.* 2 (2005) 8.
- [2] F. Watari, N. Takashi, A. Yokoyama, M. Uo, T. Akasaka, Y. Sato, S. Abe, Y. Totsuka, K. Tohji, Material nanosizing effect on living organisms: non-specific, biointeractive, physical size effects, *J. R. Soc. J. R. Soc. Interface* 6 (2009) S371–S388.
- [3] S. Hussain, L.C. Thomassen, I. Ferecatu, M.C. Borot, K. Andreau, J. a. Martens, J. Fleury, A. Baeza-Squiban, F. Marano, S. Boland, Carbon black and titanium dioxide nanoparticles elicit distinct apoptotic pathways in bronchial epithelial cells, *Part Fibre Toxicol.* 7 (2010) 10.
- [4] J. Erriquez, V. Bolis, S. Morel, I. Fenoglio, B. Fubini, P. Quagliotto, C. Distasi, Nanosized TiO₂ is internalized by dorsal root ganglion cells and causes damage via apoptosis, *Nanomedicine* 11 (2015) 1309–1319.
- [5] S. Aueviriyavit, D. Phummiratch, K. Kulthong, R. Maniratanachote, Titanium dioxide nanoparticles-mediated in vitro cytotoxicity does not induce Hsp70 and Grp78 expression in human bronchial epithelial A549 cells, *Biol. Trace Elem. Res.* 149 (2012) 123–132.
- [6] X. Chen, S.S. Mao, Titanium dioxide nanomaterials: synthesis, properties, modifications and applications, *Chem. Rev.* 107 (2007) 2891–2959.
- [7] I. Jo, S. Cho, H. Kim, B.M. Jung, S.K. Lee, S.B. Lee, Titanium dioxide coated carbon nanofibers as a promising reinforcement in aluminum matrix composites fabricated by liquid pressing process, *Scr. Mater.* 112 (2016) 87–91.
- [8] X. Wang, R.A. Gittens, R. Song, R. Tannenbaum, R. Olivares-Navarrete, Z. Schwartz, H. Chen, B.D. Boyan, Effects of structural properties of electrospun TiO₂ nanofiber meshes on their osteogenic potential, *Acta Biomater.* 8 (2012) 878–885.
- [9] D.W. Porter, N. Wu, A.F. Hubbs, R.R. Mercer, K. Funk, F. Meng, J. Li, M.G. Wolfarth, L. Battelli, S. Friend, M. Andrew, R. Hamilton, K. Sriram, F. Yang, V. Castranova, A. Holian, Differential mouse pulmonary dose and time course responses to titanium dioxide nanospheres and nanobelts, *Toxicol. Sci.* 131 (2013) 179–193.
- [10] N. Viriya-empikul, T. Charinpanitkul, S. Noriaki, A. Soottitaw, T. Kikuchi, K. Faungnawakij, W. Tanthapanichakoon, Effect of preparation variables on morphology and anatase–brookite phase transition in sonication assisted hydrothermal reaction for synthesis of titanate nanostructures, *Mater. Chem. Phys.* 118 (2009) 254–258.
- [11] M. Yurdakoç, M. Akçay, Y. Tonbul, K. Yurdakoç, Acidity of silica-alumina catalysts by amine titration using Hammett indicators and FT-IR study of pyridine adsorption, *Turk. J. Chem.* 23 (1999) 319–327.
- [12] S. Wang, H. Yu, J.K. Wickliffe, Limitation of the MTT and XTT assays for measuring cell viability due to superoxide formation induced by nano-scale TiO₂, *Toxicol. Vitr.* 25 (2011) 2147–2151.
- [13] H. Yin, P.S. Casey, Effects of aspect ratio (AR) and specific surface area (SSA) on cytotoxicity and phototoxicity of ZnO nanomaterials, *Chemosphere* 124 (2015) 116–121.
- [14] R.F. Hamilton, N. Wu, D. Porter, M. Buford, M. Wolfarth, A. Holian, Particle length-dependent titanium dioxide nanomaterials toxicity and bioactivity, *Part. Fibre Toxicol.* 6 (2009) 35.
- [15] K. Donaldson, F.A. Murphy, R. Duffin, C.A. Poland, Asbestos, carbon nanotubes and the pleural mesothelium: a review of the hypothesis regarding the role of long fibre retention in the parietal pleura, inflammation and mesothelioma, *Part. Fibre Toxicol.* 7 (2010) 5.
- [16] T. Morishige, Y. Yoshioka, A. Tanabe, X. Yao, S.I. Tsunoda, Y. Tsutsumi, Y. Mukai, N. Okada, S. Nakagawa, Titanium dioxide induces different levels of IL-1β production dependent on its particle characteristics through caspase-1 activation mediated by reactive oxygen species and cathepsin B, *Biochem. Biophys. Res. Commun.* 392 (2010) 160–165.
- [17] S. Hussain, S. Boland, A. Baeza-Squiban, R. Hamel, L.C.J. Thomassen,

- J.A. Martens, M.A. Billon-Galland, J. Fleury-Feith, F. Moisan, J.C. Pairon, F. Marano, Oxidative stress and proinflammatory effects of carbon black and titanium dioxide nanoparticles: role of particle surface area and internalized amount, *Toxicology* 260 (2009) 142–149.
- [18] N. Viriya-empikul, S. Noriaki, T. Charinpanitkul, T. Kikuchi, W. Tanthapanichakoon, A step towards length control of titanate nanotubes using hydrothermal reaction with sonication pretreatment, *Nanotechnology* 19 (2008) 035601.
- [19] M. Xu, J. Li, H. Iwai, Q. Mei, D. Fujita, H. Su, H. Chen, N. Hanagata, Formation of nano-bio-complex as nanomaterials dispersed in a biological solution for understanding nanobiological interactions, *Sci. Rep.* 2 (2012) 1–6.
- [20] R.A. French, A.R. Jacobson, B. Kim, S.L. Isley, L. Penn, P.C. Baveye, Influence of ionic strength, pH, and cation valence on aggregation kinetics of titanium dioxide nanoparticles, *Environ. Sci. Technol.* 43 (2009) 1354–1359.
- [21] K. Suttiponparnit, J. Jiang, M. Sahu, S. Suvachittanont, T. Charinpanitkul, P. Biswas, Role of surface area, primary particle size, and crystal phase on titanium dioxide nanoparticle dispersion properties, *Nanoscale Res. Lett.* 6 (2011) 1–8.
- [22] A. Bidani, C.Z. Wang, S.J. Saggi, T.A. Heming, Evidence for pH sensitivity of tumor necrosis factor-alpha release by alveolar macrophages, *Lung* 176 (1998) 111–121.